JOURNAL OF AGRICULTURAL AND FOOD CHEMISTRY

Metabolism of Fungicide Diethofencarb in Grape (*Vitis vinifera* L.): Definitive Identification of Thiolactic Acid Conjugated Metabolites

TAKUO FUJISAWA,*,† KEIKO ICHISE-SHIBUYA,† TOSHIYUKI KATAGI,† LUIS O. RUZO,§ AND YOSHIYUKI TAKIMOTO†

Environmental Health Science Laboratory, Sumitomo Chemical Co., Ltd., 2-1, Takatsukasa 4-Chome, Takarazuka 665-8555, Japan, and PTRL West, Inc., 625-B Alfred Nobel Drive, Hercules, California 94547

The metabolic fate of diethofencarb (isopropyl 3,4-diethoxycarbanilate) separately labeled with ^{14}C at the phenyl ring and 2-position of the isopropyl moiety was studied in grape (*Vitis vinifera* L.). The acetonitrile solution of ^{14}C-diethofencarb at a rate of 500 g a.i. ha^{-1} was once applied topically to fruits or leaves at the maturity stage of fruits (PHI 35 days), and the plants were grown in the greenhouse until harvest. In the grape plants, diethofencarb was scarcely translocated to the untreated portion and was degraded more in the fruit as compared to the leaf. For the fruit, diethofencarb primary underwent *O*-deethylation at the 4-position of the phenyl ring to form the phenolic derivative, isopropyl 3-ethoxy-4-hydroxycarbanilate (0.9% of the total radioactive residue, TRR). This metabolite was successively transformed via conjugation with glucose at the phenolic hydroxy group (8.1−18.1% TRR) or with thiolactic acid at the 5-position of the phenyl ring (1.5−1.7% TRR). The thiolactic acid conjugate was further metabolized mainly to two different types of glucose conjugates at the 4-position of the phenyl ring (8.7−13.5% TRR) and the hydroxy group in the thiolactic acid moiety (6.4−7.3% TRR), as evidenced by ^1H NMR and atmospheric pressure chemical ionization−liquid chromatography−mass spectrometry together with cochromatographies with synthetic standards.

KEYWORDS: Diethofencarb; metabolism; *Vitis vinifera* L.; conjugate; thiolactic acid

INTRODUCTION

The carbamate fungicide diethofencarb (**1**) (isopropyl 3,4-diethoxycarbanilate) is very effective for the control of various fungal species, especially *Botrytis* sp., *Cercospora* sp., and *Venturia* sp., which are resistant to benzimidazole fungicide (*1*−*3*). The metabolic fate of *N*-aryl carbamates in various plants has been extensively studied especially for herbicides chlorpropham (isopropyl 3-chlorocarbanilate) and propham (isopropyl carbanilate). James and Prendeville (*4*) have reported that chlorpropham treated on leaf is extensively converted to water soluble metabolites in smartweed, pigweed, and tomato, which are susceptible to chlorpropham. These water soluble fractions were supposed to consist of β-glucose derivatives conjugated at the 1-hydroxyprop-2-yl moiety of the primary metabolite. In hydroponically grown soybean, polar metabolites were detected in both roots and shoots (*5*). Isopropyl 5-chloro-2-hydroxycarbanilate (2-OH-chlorpropham) was identified as an aglycone in both roots (*6*) and shoots (*7*), and isopropyl 3-chloro-4-hydroxycarbanilate (4-OH-chlorpropham) was in the shoot only (*7*). In cucumber, potato, and oat, chlorpropham was found to be metabolized only to 4-OH-chlorpropham (*8*−*10*). Especially, Still et al. have found in oat metabolism of chlorpropham that cysteine is attached to the phenyl ring of 4-OH-chlorpropham by the C−S linkage (*9*). Propham has been shown to be metabolized via ring hydroxylation in several plant species. The only aglycone identified in soybean when treated with β-glucosidase was isopropyl 2-hydroxycarbanilate (2-OH-propham), produced by roots and shoots (*11*). In alfalfa, isopropyl 4-hydroxycarbanilate (4-OH-propham) and 2-OH-propham were identified as major and minor aglycones, respectively, in the shoot and the root (*12*). Zurqiyah et al. have shown that hydroxylation and conjugation are important transformation routes in the metabolism of propham in alfalfa (*13*). In the shoots, hydroxylation on the isopropyl moiety occurred to an equal extent with hydroxylation on the 2- and 4-positions of the phenyl ring.

Diethofencarb can be classified into the carbanilate pesticides and possesses the electron-donating ethoxy groups in the phenyl ring different from chlorpropham and propham; hence, the different types of metabolism could be supposed in plants. From this standpoint, we have conducted metabolism of **1** in grape grown in a greenhouse and attempted to identify the metabolites by extensive spectrometric analysis of plant extracts using liquid chromatography−mass spectrometry (LC-MS) and

* Corresponding author (e-mail: fujisawat1@sc.sumitomo-chem.co.jp).
† Sumitomo Chemical Co., Ltd..
§ PTRL West, Inc..

10.1021/jf034367+ CCC: $25.00
Published on Web 07/25/2003

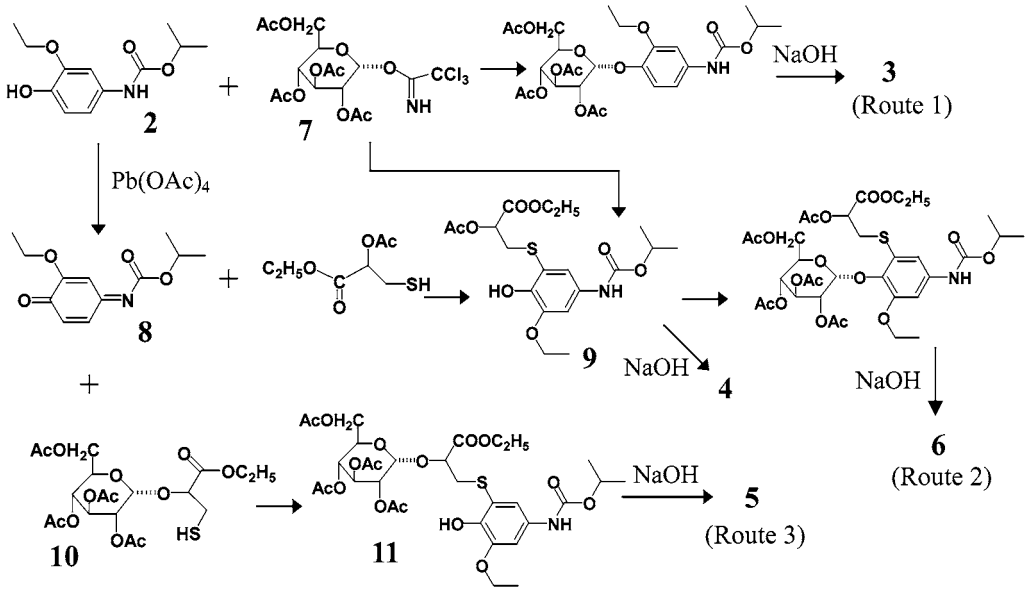

Figure 1. Synthetic routes of authentic standards **3**–**6**.

nuclear magnetic resonance (NMR) spectrometry in conjunction with direct chromatographic comparison with the synthetic standards.

MATERIALS AND METHODS

Chemicals. The nonradiolabeled synthetic standards, **1**, its *O*-deethylated derivative at the 4-position of the phenyl ring (isopropyl 3-ethoxy-4-hydroxycarbanilate, **2**), the glucose conjugate of **2** (isopropyl 3-ethoxy-4-β-glucopyranosyloxycarbanilate, **3**), the thiolactic acid conjugate of **2** (3-{3-ethoxy-2-hydroxy-5-[(isopropoxycarbonyl)amino]-phenylthio}-2-hydroxypropionic acid, **4**), and the two glucose conjugates of **4** (3-{3-ethoxy-2-hydroxy-5-[(isopropoxycarbonyl)amino]-phenylthio}-2-β-glucopyranosyloxypropionic acid, **5**, and 3-{3-ethoxy-2-β-glucopyranosyloxy-5-[(isopropoxycarbonyl)amino]phenylthio-2-hydroxypropionic acid}, **6**) were synthesized in our laboratory. The synthetic routes of **3**−**6** are briefly shown in **Figure 1**. All intermediates were purified by silica gel column chromatography except for the unstable quinoneimine derivative **8**. 3,4-Diethoxynitrobenzene prepared by reaction of 4-nitrocatechol in dioxane with 3.0 equiv of ethyl iodide in the presence of 1.05 equiv of sodium hydride was hydrolyzed by potassium hydroxide in aqueous 2-methoxy ethanol under reflux to give 3-ethoxy-4-hydroxy-nitrobenzene (*14*). The catalytic reduction of this nitrobenzene derivative by 10% Pd−C under hydrogen atmosphere produced the corresponding aniline, which was subsequently coupled with isopropyl chloroformate (1.5 equiv) in dimethyl formamide in the presence of 0.2 equiv *N*,*N*-dimethylaniline leading to formation of **2** (total yield, ~30%) (*2*). The trichloromethylimidate derivative **7** was separately prepared from tetraacetylglucose, which was prepared by treating tetraacetyl-1-bromo-glucose and $AgCO_3$ with 1,1,1-trichloromethyl cyanide (10 equiv) in dichloromethane. By coupling **2** and **7** in dichloromethane (*15*), the tetraacetylglucose derivative of **2** was obtained and hydrolyzed by sodium hydroxide to afford **3** (total yield 67.0%, route 1). Along with the route 2 (**Figure 1**), ethyl bromolactate was first prepared by reduction of ethyl bromopyruvate with 0.3 equiv of $NaBH_4$ in ethanol. Its hydroxy group was subsequently acetylated in the usual manner, followed by reaction with *N*,*N*-dimethylthioformamide (Me_2NCHS) to give the corresponding ethyl mercaptolactate (*16*). Compound **2** in dry dichloromethane was oxidized by lead acetate to form the corresponding quinoneimide derivative **8** (*17*) and then coupled with ethyl mercaptolactate to synthesize **9** (*18*). A portion of **9** was hydrolyzed with sodium hydroxide to yield **4**. Another portion of **9** was then reacted with **7** in dichloromethane and subsequently hydrolyzed by sodium hydroxide to **6** (total yield, 45.4%). To synthesize **5** via route 3, the pentaacetylglucose was first coupled with ethyl bromolactate in the presence of trifluoroborane−diethyl ether complex (5.0 equiv) to prepare the tetraacetyl-1-bromoglucose derivative, which was subsequently treated with Me_2NCHS in the similar manners of route 1. The obtained glucose derivative **10** was coupled with **8** to synthesize **11**, which was hydrolyzed to **5** (total yield, 13.6%). The chemical structures of the authentic standards **2**−**6** were confirmed by ^{1}H NMR and LC-MS, as listed in **Table 1**, and their high-performance liquid chromatography (HPLC) retention times and thin-layer chromatography (TLC) R_f values are listed in **Table 2**.

Compound **1** uniformly labeled with ^{14}C at the phenyl ring [^{14}C-phenyl] or at the 2-position of the isopropyl moiety [^{14}C-isopropyl] was prepared in our laboratory and had a specific activity of 8.88 and 7.64 MBq mg^{-1}, respectively. Their radiochemical purity was more than 98% as determined by HPLC. Cellulase (EC 3.2.1.4) purchased from Wako Pure Chemical Industries Ltd. (Osaka) were used for enzymatic hydrolysis of sugar conjugates. Other reagents were of the purest grade commercially available.

Spectroscopies. ^{1}H NMR spectra were measured with a Varian Unity 300 FT-NMR spectrometer operating at 299.94 MHz with 4-Nucleus auto NMR probe, using trimethylsilylpropionate-2,2,3,3-d_4 as an internal standard (δ = 0.0 ppm). LC−atmospheric pressure chemical ionization−MS (LC-APCI-MS) in positive and negative ion modes was performed using a Hitachi M-1000 spectrometer equipped with a Hitachi 6000 series liquid chromatography. Samples dissolved in methanol were manually injected into an APCI source at 260 °C through an ODS column with a flow rate of 1.0 mL min^{-1} using a gradient system with acetonitrile (solvent A) and 0.1% formic acid in water (solvent B). The composition of the mobile phase was changed stepwise as follows: 0 min, %A−%B, 25−75; 60 min, %A−%B, 50−50 (method 1); 0 min, %A−%B, 50−50; 30 min, %A−%B, 100−0 (method 2).

Radioassay. Radioactivity in the liquid extracts and the surface rinse from plants was determined by mixing each aliquot with 10 mL of Packard Scintillator Plus and analyzed by liquid scintillation counting (LSC) with Packard model 1600TR and 2000CA spectrometers equipped with an automatic external standard. The background level of radioactivity in LSC was 30 dpm in an average, which was subtracted from the dpm value of a measured sample. Radioactivity in the unextractable residues from the treated plants was measured by using a Packard model 306 Sample Oxidizer. Unextractable residues were air-dried at room temperature overnight and weighed with a Mettler model AE240, and each aliquot was subjected to combustion. $^{14}CO_2$ produced was absorbed into 9 mL of Packard Carb-CO_2 absorber and mixed with 15 mL of Packard Permafluor scintillator, and the radioactivity in it was quantified by LSC. The efficiency of combustion was determined to be greater than 90%.

Chromatographies. HPLC was carried out by using a Hitachi L-6200 Pump linked in series with L-4000 UV detector and Packard

Table 1. NMR and MS Data of Authentic Standards

	^{1}H NMR (ppm)	MS (*m*/*z*)
2	1.28 (d, J = 6 Hz, 6H; $(CH_3)_2CH$), 1.43 (t, J = 6 Hz, 3H; CH_3CH_2), 4.11 (q, J = 6 Hz, 2H; CH_3CH_2), 4.99 (m, J = 6 Hz, 1H; $(CH_3)_2CH$), 5.42 (s, 1H; OH), 6.40 (br-s, 1H; NH), 6.45–7.00 (m, 3H; aromatic-H)	240 $(M + H)^+$, 226, 198
3	1.29 (d, J = 6 Hz, 6H; $(CH_3)_2CH$), 1.42 (t, J = 6 Hz, 3H; CH_3CH_2), 4.11 (q, J = 6 Hz, 2H; CH_3CH_2), 4.99 (m, J = 6 Hz, 1H; $(CH_3)_2CH$), 3.10–4.60 (m, 7H; sugar-H), 6.86–7.20 (m, 3H; aromatic-H)	400 $(M - H)^-$, 238
4	1.30 (d, J = 6 Hz, 6H; $(CH_3)_2CH$), 1.44 (t, J = 6 Hz, 3H; CH_3CH_2), 3.20 (d, J = 6 Hz, 2H; CH_2CH), 4.13 (q, J = 6 Hz, 2H; CH_3CH_2), 4.32 (t, J = 3 Hz, 1H; CH_2CH), 4.97 (m, 1H; $(CH_3)_2CH$), 6.95–7.05 (s, 2H; aromatic-H)	358 $(M - H)^-$, 313
5	1.28 (d, J = 6 Hz, 6H; $(CH_3)_2CH$), 1.43 (t, J = 6 Hz, 3H; CH_3CH_2), 4.11 (q, J = 6 Hz, 2H; CH_3CH_2), 4.30 (t, J = 6 Hz, 1H; CH_2CH), 4.98 (m, J = 6 Hz, 1H; $(CH_3)_2CH$), 3.10–4.60 (m, 7H; sugar-H and d, 2H; CH_2CH), 7.00–7.10 (s, 2H; aromatic-H)	520 $(M - H)^-$, 340, 270
6	1.28 (d, J = 6 Hz, 6H; $(CH_3)_2CH$), 1.42 (t, J = 6 Hz, 3H; CH_3CH_2), 4.12 (q, J = 6 Hz, 2H; CH_3CH_2), 4.34 (t, J = 6 Hz, 1H; CH_2CH), 4.99 (m, J = 6 Hz, 1H; $(CH_3)_2CH$), 3.10–4.60 (m, 7H; sugar-H and d, 2H; CH_2CH), 7.00–7.10 (s, 2H; aromatic-H)	520 $(M - H)^-$

Table 2. HPLC Retention Times and TLC R_f Values of Synthetic Standards

	retention time (min)	R_f value	
compd	method 1	system 1[a]	system 2[b]
1	66.6	0.63	0.73
2	50.3	0.57	0.72
3	35.1	0.07	0.55
4	46.0	0.28	0.53
5	39.7	0.03	0.32
6	34.7	0.02	0.28

[a] Toluene/ethyl formate/formic acid = 5/7/1 (v/v/v). [b] Butanol/acetic acid/water = 6/1/1 (v/v/v).

Flow-one/Beta A-120 radio detector equipped with a 500 μL liquid cell where Ultima-Flo AP (Packard) was utilized as a scintillator. A Sumipax ODS A-212 column (150 mm × 6 mm i.d., 5 μm, SCAS Co., Ltd.) was employed for both analytical and preparative purposes at a flow rate of 1 mL min^{-1}, and a YMC-Pack AM-324 S-5 120A ODS column (300 mm × 10 mm i.d., 5 μm, YMC Co., Ltd.) was used for a preparative purpose at a flow rate of 2 mL min^{-1}. The following gradient system was used for typical analysis of the metabolites with 0.01% trifluoroacetic acid (solvent A) and acetonitrile (solvent B): 0 min, %A−%B, 95−5; 60 min, %A−%B, 50−50; 60.1 min, %A−%B, 0−100; 80 min, %A−%B, 0−100 (method 3). The following HPLC methods (methods 4 and 5) and/or their slightly modified ones were used for separation and purification of metabolites: YMC-Pack AM-324; 0.01% trifluoroacetic acid (solvent A) and acetonitrile (solvent B); 0 min, %A−%B, 75−25; 60 min, %A−%B, 50−50; 60.1 min, %A−%B, 0−100; 80 min, %A−%B, 0−100 (method 4); YMC-Pack AM-324; 1/33M phosphate buffer (solvent A) and acetonitrile (solvent B); 0 min, %A−%B, 85−15; 25 min, %A−%B, 85−15; 25.1 min, %A−%B, 50−50; 45 min, %A−%B, 50−50 (method 5).

TLC was conducted using silica gel 60 F_{254} thin-layer chromatoplates (20 cm × 20 cm, 0.25 mm thickness, E. Merck). The following solvent systems were used for development: toluene/ethyl formate/formic acid, 5/7/1 (v/v/v); *n*-butanol/acetic acid/water, 6/1/1 (v/v/v). The nonradiolabeled reference standards were detected by exposing TLC plates to ultraviolet light. Autoradiograms were prepared by exposing TLC plates to BAS-IIIs Fuji Imaging Plate for several hours. The radioactivity on an imaging plate was detected by using a Fuji Bio-Imaging Analyzer BAS-1500.

Plant Material, Maintenance, and Treatment. For investigation of metabolic profiles, grape vines (*Vitis vinifera* L., cv. Kyoho) with fruits setting at maturity stages were purchased from Takii & Co., Ltd. The grape plants were grown in pots in a greenhouse with the temperature maintained at 25 °C for day and 20 °C for night. The plant was appropriately watered until harvest for approximately 1.5 months. [^{14}C]-**1** in the following solutions was topically applied at a rate of 500 g a.i. ha^{-1} to grape bunches (fruits) and leaves once with a preharvest interval (PHI) of 35 days. The acetonitrile solutions of [^{14}C-phenyl] and [^{14}C-isopropyl]-**1** isotopically diluted by 10−15-fold with nonradiolabeled **1** were prepared at the concentrations of 2.85−4.00 mg mL^{-1} for fruit and leaf treatments. The surface area of the grape bunch was conveniently calculated to be 114 cm^2 by assuming its shape as a circular cone (radius of the bottom circle, 5 cm; height, 12 cm). The surface area of the leaf was geometrically estimated to be 78.5 cm^2 on average. [^{14}C]-**1** was topically applied to the surface of fruits on each bunch and leaves using a microsyringe. Six bunches and seven leaves per pot were treated with each label. The application was conducted when the color of the skin began to change (verasion).

For the purpose of collecting enough conjugated metabolites subjected to spectrometric analyses (MS, NMR), Pinot Noir grapes under the actual field conditions were used. The field phase of this study was carried out at Valley Farm Management, 37500 Foothill Drive, Soledad, CA. [^{14}C-Phenyl]-**1** in the following solutions was applied to the grape bunches with a hand sprayer at a rate of 1000 g a.i. ha^{-1}, three times with an approximately 40 days interval. For preparation of dose solution, [^{14}C-phenyl]-**1** was isotopically diluted by 2-fold with nonradiolabeled **1**. For each application, the grape bunches of five vines (130 bunches) were sprayed with 175 mg of [^{14}C-phenyl]-**1** (4.4 MBq) dissolved in 75 mL of methanol/water (1/1, v/v). The surface area of the grape bunch (cm^2) before application was approximately calculated as 3 in. × 6 in., which was equal to an area of 18 square inches per bunch. The first, second, and third applications were conducted at the stage of late fruit setting, beginning of fruit verasion, and fruit verasion, respectively. PHI was set as 14 days. There was no irrigation carried out during the actual field phase of this study.

Extraction and Isolation of Metabolites. For investigation of the metabolic profiles, the grape bunches applied with [^{14}C]-**1** were sampled at 35 days after the treatment. The harvested samples were weighed and stored in a freezer (< −20 °C) until analysis was conducted. After the surface of bunches was rinsed by methanol (100 mL per bunch), grape fruits were removed from the bunches by using scissors, homogenized in a homogenizer (Nissei, AM-8) at 10 000 rpm for 10 min, and centrifuged (Tomy, CX250) at 5000 rpm for 10 min to separate supernatant (juice) and pulp. The supernatant was filtered through a filter paper (pore size; 1 μm) to remove the precipitate. The pulp was further extracted in the homogenizer (10 000 rpm, 10 min) by acetone/water (4/1, v/v) at the ratio of 2 mL per 1 g of pulp. The mixture was filtered, and the residue was extracted two additional times in the same way. The aliquots of surface rinse, juice, and pulp extracts were individually radioassayed with LSC and analyzed by HPLC and TLC cochromatographies with authentic standards. Pulp residues were air-dried in open vessels at room temperature overnight, and subsamples of the dried residues were subjected to combustion analysis to determine the remaining radioactivity. The untreated leaves were also sampled to examine the extent of translocation of radioactivities. They were chopped, air-dried in a chamber at room temperature for 1 week, and subjected to combustion.

Grape leaves applied with [^{14}C]-**1** were also sampled at 35 days after the treatment. The grape leaves were surface rinsed by methanol (100 mL) to remove external radioactivity, cut into small pieces, and similarly homogenized as fruits at the ratio of 20 mL per 1 g of the plant material. The mixture was filtered through a filter paper, and the residue was extracted two additional times in the same way. The extract and surface rinse were radioassayed and then individually concentrated to dryness, redissolved in a small volume of organic solvent, and each aliquot was subjected to HPLC and TLC analyses. Unextractable residues and untreated leaves were air-dried and combusted with the sample oxidizer prior to LSC analysis.

For the purpose of collecting enough amount of conjugated metabolites, grape fruits applied with [^{14}C-phenyl]-**1** in the field were sampled at 14 days after the last treatment. The harvested samples were weighed and stored in a freezer (< −20 °C) until analysis was conducted. While still frozen, bunches were rinsed with acetone followed by acetone/water (9/1, v/v). Bunches were allowed to thaw, and grape fruits were removed from bunches to crush by hand. The grape juice and pulp were separated through a funnel and glass wool plug. All of the juice was combined (1.5 L) and subjected to preparative purification by the solid phase absorbent Porapack Q. Approximately 300 mL of juice was loaded on the Porapack Q column packed in a glass Econo-column (50 cm × 5 cm) to a height of 30 cm, and the column was successively washed with 900 mL of water, 5 and 50% acetonitrile in water, and acetonitrile. These procedures were repeated five times, and each of four fractions (4.5 L) was separately combined for LSC and HPLC analysis, indicating that most of the unknown metabolites was eluted in the third fraction. The third fraction concentrated to remove acetonitrile was further fractionated on the Porapack Q column by successive elutions with 750 mL of aqueous acetonitrile with more gradual solvent gradient (0, 1, 5, 10, 15, 25, 35, 50, and 100% acetonitrile in water). The fifth and sixth fractions (15−25% acetonitrile) were combined and subjected to the repeated purification using HPLC by methods 3−5.

Identification of Metabolites. The major unknown metabolites were subjected to enzymatic hydrolysis (cellulase, 37 °C, overnight) in 10 mM phosphate buffer at pH 5. Separately, they were isolated from grape fruits and subjected to LC-APCI-MS and NMR analyses. Acetylation was conducted by treating the isolated metabolites with anhydrous acetic acid in the trace amount of dry pyridine, and methylation was conducted by putting droplets of trimethylsilyldiazomethane into metabolite dissolved in methanol/dichloromethane (1/1, v/v), according to the usual manners. Acetylated and methylated unknown metabolites were also subjected to LC-APCI-MS and NMR analyses. Finally, the identity of the unknown metabolites was confirmed by HPLC and TLC cochromatographies with nonradiolabeled reference standards.

RESULTS

Distribution of Metabolites. In the case of fruit and leaf treatments at a rate of 500 g a.i. ha^{-1}, the recovered radioactivity was 73.0−77.2 and 77.3−78.7% of the applied ^{14}C, respectively. The radioactive residues in untreated leaves with the fruit treatment were less than 0.01% of the applied ^{14}C (1 ppb), and those in untreated leaves and fruits were less than 0.01% (0.01 ppm) when the leaf was treated. These results indicated the insignificant translocation of radioactivity from treated portions, and the unrecovered ^{14}C at harvest was likely to be lost by vaporization.

Distribution of radioactivity and metabolites in the surface rinse, juice, and pulp in fruit treated with [^{14}C]-**1** at a rate of 500 g a.i. ha^{-1} is summarized in **Table 3**. No typical difference in distribution was observed between the two radiolabels. Most of the radioactivity in the surface rinse remained as intact **1** (50.7−55.0% total radioactive residue, TRR). Metabolites such as **2**−**6** were mainly detected from juice and pulp extracts. Within the whole grape, **1** remained as the major residue (52.8−60.9% TRR). Major metabolites detected were **3** (8.1−18.1% TRR, 0.153−0.289 ppm), **5** (6.4−7.3% TRR, 0.102−0.137 ppm), and **6** (8.7−13.5% TRR, 0.165−0.216 ppm). Minor metabolites **2** and **4** were both detected below 1.7% TRR. Meanwhile, the distribution of radioactivity from the treated leaves was different from that of the fruits (**Table 4**). Most of the radioactivity in the surface rinse remained as intact **1** (94.9−95.1% TRR). Metabolites such as **3** and **5** were mainly detected from the extract. Within the whole leaf, **1** was major residue

Table 3. Distribution of Radioactivities and Metabolites of [^{14}C]-**1** with Fruit Treatment

	[^{14}C-phenyl]-**1**		[^{14}C-isopropyl]-**1**	
	%TRR	ppm[a]	%TRR	ppm[a]
		surface rinse		
1	50.71	0.811	54.98	1.038
others	ND	ND	0.57	0.011
		juice		
1	ND	ND	1.61	0.030
2	ND	ND	ND	ND
3	13.46	0.215	5.41	0.102
4	ND	ND	ND	ND
5	3.29	0.053	3.97	0.075
6	9.76	0.156	6.51	0.123
others	2.73	0.044	7.04[b]	0.133[b]
		pulp extract		
1	2.04	0.033	4.28	0.081
2	0.90	0.014	ND	ND
3	4.60	0.074	2.70	0.051
4	1.51	0.024	1.68	0.032
5	3.10	0.050	3.28	0.062
6	3.72	0.060	2.20	0.042
others	3.57[c]	0.057[c]	1.07[d]	0.020[d]
unextractable	0.61	0.010	4.68	0.088
		untreated leaf		
	<0.01	0.001	<0.01	0.001
		total		
	100.00	1.599	100.00	1.888

[a] ppm of **1** equivalent. [b] Consisted of more than four metabolites, each metabolite below 3.70% TRR (0.070 ppm). [c] Consisted of more than eight metabolites, each metabolite below 0.80% TRR (0.013 ppm). [d] Consisted of more than two metabolites, each metabolite below 0.57% TRR (0.010 ppm).

Table 4. Distribution of Radioactivities and Metabolites of [^{14}C]-**1** with Leaf Treatment

	[^{14}C-phenyl]-**1**		[^{14}C-isopropyl]-**1**	
	%TRR	ppm[a]	%TRR	ppm[a]
		surface rinse		
1	94.90	75.741	95.07	61.180
others	ND	ND	0.55	0.349
		extract		
1	0.65	0.516	0.73	0.466
2	ND	ND	ND	ND
3	0.49	0.391	ND	ND
4	ND	ND	ND	ND
5	0.57	0.458	0.43	0.273
6	ND	ND	ND	ND
others	2.33[a]	1.856[a]	2.53[b]	1.620[b]
unextractable	1.06	0.847	0.69	0.444
		untreated leaf		
	<0.01	<0.010	<0.01	<0.010
		untreated fruit		
	ND	ND	ND	ND
		total		
	100.00	79.809	100.00	64.332

[a] ppm of **1** equivalent. [b] Consisted of more than 17 metabolites, each metabolite below 0.46% TRR (0.367 ppm). [c] Consisted of more than eight metabolites, each metabolite below 0.55% TRR (0.348 ppm).

(95.6−95.8% TRR) and the amounts of metabolites **3** and **5** were less than 0.6% TRR. These results indicated more penetration of **1** followed by metabolic degradation in fruits as compared with leaves.

Identification of Metabolites 2 and 3. The chemical structure of **2** was easily confirmed by HPLC and TLC cochromatographies of the isolated metabolite with the synthetic standard. In the case of **3**, the corresponding HPLC fraction of extracts was collected and divided into two portions. One portion was incubated with cellulase, and a new peak corresponding to **2** appeared via concomitant decrease of the peak due to **3**. The formation of **2** as an aglycone was also confirmed by two-dimensional TLC cochromatography with the authentic standard. To further investigate the chemical nature of **3**, the remaining portion was subjected to LC-APCI-MS analysis in a negative ion mode. Metabolite **3** was shown to have a molecular weight of 401, as evidenced from the MS peak at *m*/*z* 400 ($[M - H]^-$). These results strongly suggest glucose, or equivalent, as the conjugation moiety. Definitive identification of **3** was achieved by synthesizing the glucose conjugate of **2** and carrying out direct comparison of the isolated **3** with this synthetic standard by HPLC and TLC cochromatographies.

Identification of Metabolites 4 and 5. Metabolite **5** was incubated with cellulase, and a new peak corresponding to **4** appeared via concomitant decrease of the peak due to **5**. The formation of **4** was also confirmed by two-dimensional TLC cochromatography with the authentic standards. LC-APCI-MS analysis in a negative ion mode showed that the molecular weight of **5** isolated from the extracts was most likely to be 521, as demonstrated by the MS peak at *m*/*z* 520 $[M - H]^-$. The methylation of **5** was attempted by using trimethylsilyldiazomethane, and the resultant product was subjected to LC-APCI-MS in a negative ion mode. The introduction of the two methyl groups was shown by the MS peak at *m*/*z* 548 $[M - H]^-$. When **5** was acetylated by the usual manners, the MS peak at *m*/*z* 730 $[M - H]^-$ was observed, indicating the introduction of five acetyl groups into the molecule. To estimate the functional groups of **5** in detail, the successive derivatization (methylation followed by acetylation) was conducted. LC-APCI-MS in a negative ion mode showed the MS peak at *m*/*z* 716 $[M - H]^-$; hence, the two methyl and four acetyl groups were formed to be added to the molecule. Assuming that the aglycone of **5** is **2**, one methyl group may be introduced via methylation of the activated phenol at the 4-position, while the other one may be introduced from methylation of a carboxylic acid functionally associated with a conjugating moiety. The acetyl groups introduced are probably due to hydroxy functionalities of a monosaccharide, which is also consistent with observed molecular weight. The NMR spectrum of the methylated derivative of **5** was measured as shown in **Figure 2**. Only two aromatic protons were observed at 6.95 and 7.05 ppm with the coupling constant of 2.0 Hz, indicating the presence of two aromatic protons in the *meta*-position; hence, some metabolic conversion at the 5-position of the phenyl ring was most likely. By the way, the isopropyl and one ethoxy groups were found to remain intact. The methyl groups appeared as a doublet at 1.25 ppm with an accompanying isopropyl proton at 5.00 ppm, and the ethoxy protons at 1.40 (triplet) and 4.05 ppm (quartet) were also present. A large number of coupled resonance possibly due to glucopyranosyl protons appeared at 3.10−4.60 ppm, secondary hydroxyl groups, implying that **5** was a sugar conjugate. The two sharp singlets appeared at 3.75 and 3.80 ppm due to methylation of **5**, possibly implying the presence of the methyl ester and methoxy groups and, hence, the formation of a more complex conjugate than a simple sugar derivative. Taking into account all of the spectrometric evidence together with the conjugation form of other pesticides (*19*−*22*), the chemical structure of **5** was proposed. Finally, the chemical identity of **5** as 3-{3-ethoxy-2-hydroxy-5-[(isopropoxycarbonyl)-amino]phenylthio}-2-*β*-glucopyranosyloxypropionic acid was definitely confirmed by both HPLC and TLC cochromatographies with the reference standard as prepared by the route 3 in **Figure 1**.

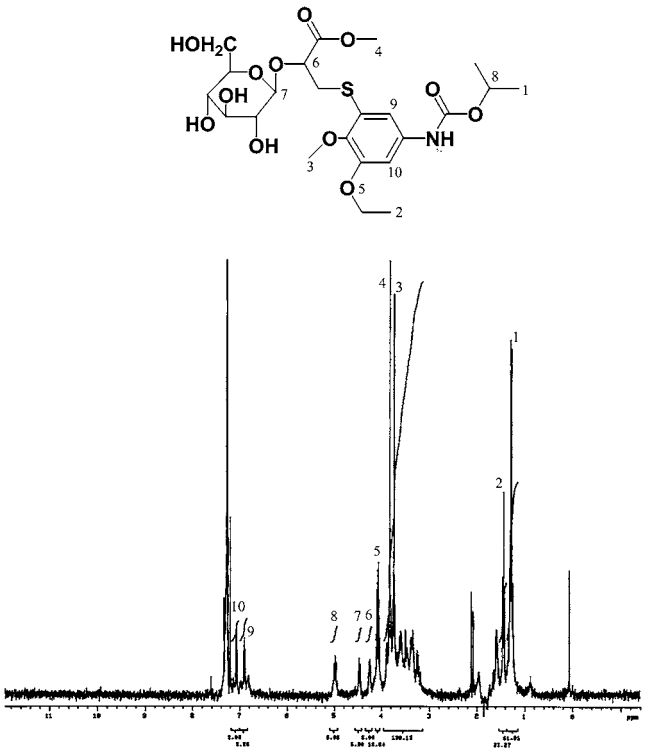

Figure 2. ^{1}H NMR spectrum of methylated **5** (3-{3-ethoxy-2-hydroxy-5-[(isopropoxycarbonyl)amino]phenylthio}-2-*β*-glucopyranosyloxypropionic acid). Metabolite **5** was isolated from grape fruits.

Considering the metabolic pathway, **4** was assumed to exist in grape as an intermediate metabolite of **5**. Therefore, the synthetic standard of **4** was used to confirm its existence in the extract of grape by HPLC and TLC cochromatographies. As a result, the metabolite corresponding to **4** was detected in grape fruit.

Identification of Metabolite 6. Metabolite **6** was incubated with cellulase; however, no degradation of **6** was observed. The LC-APCI-MS spectrum of the purified **6** in a negative ion mode showed the same molecular weight as **5** (*m*/*z* 520 $[M - H]^-$), indicating isomeric structure. LC-MS analysis in a negative ion mode showed the MS peak of the methylated **6** at *m*/*z* 534 ($[M - H]^-$) and that of methylated and acetylated derivative of **6** at *m*/*z* 744 ($[M - H]^-$). The molecular weight of the latter derivative indicated the addition of five acetyl unites to the methylated molecule. These results together with the data on metabolite **5** implied that **6** was a monosaccharide derivative, but only four acetyl groups were possibly to be introduced. Therefore, the metabolite should have an additional center sensitive to acetylation (hydroxy group of thiolactic acid attached to benzene ring via C−S bond). Considering all of the above spectrometric evidence and taking the chemical structure of **5** into account, the possible chemical structure of **6** was 3-{3-ethoxy-2-*β*-glucopyranosyloxy-5-[(isopropoxycarbonyl)amino]-phenylthio-2-hydroxypropionic acid}], which was definitely confirmed by both HPLC and TLC cochromatographies with

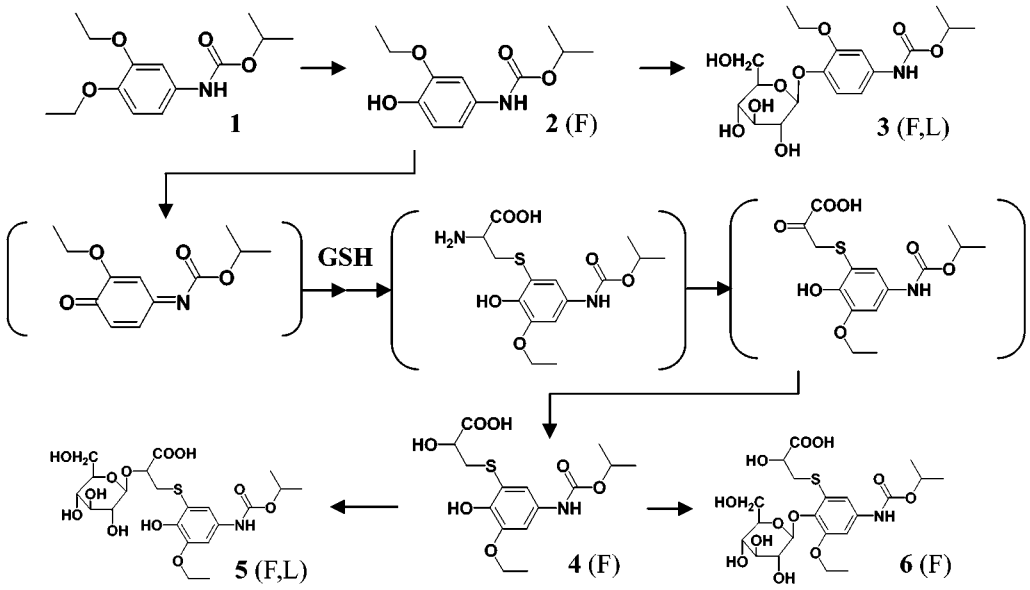

Figure 3. Proposed metabolic pathway of **1** in the grape plants. F, fruit treatment; L, leaf treatment.

the synthetic standard. On the basis of these results, the metabolic pathway of **1** in grape plants is proposed in **Figure 3**.

DISCUSSION

A great difference in the metabolic pattern of **1** was observed between the fruit and the leaf treatments. The test compound (**1**) was less degraded in the leaf while it was extremely metabolized mainly to conjugated products in the fruit. This may be, at least in part, due to the difference in the amounts and the kinds of waxes existing on the surface of plant, which affect the penetration of compound to the inner cell where the various metabolism by enzymes actually occurs. Furthermore, the difference in distribution of metabolic enzymes may exist as fruit and leaf are compared.

The mechanism on formation of the thiolactic acid conjugate was postulated from the various works conducted with acetaminophen (*N*-acetyl-*p*-aminophenol). Acetaminophen is a widely used analgesic medicine, which has *p*-aminophenol as a fundamental chemical structure. The *p*-aminophenol moiety is considered to undergo two electron oxidation, and it is easily transformed to a highly reactive benzoquinoneimine. The in vitro oxidation of acetaminophen has been extensively investigated using various enzymes such as cytochrome P-450, prostaglandin H synthase (PHS), and peroxidase (*23*−*29*), and the three possible routes to generate benzoquinoneimine from *p*-aminophenol by enzymatic oxidation was postulated. First, acetaminophen is oxidized with peroxidase or PHS via one electron oxidation to produce *N*-acetyl-*p*-benzosemiquinoneimine and the resulting semiquinoneimine is disproportionated to give acetaminophen and *p*-benzoquinoneimine. Second, acetaminophen is oxidized with P-450 and PHS directly via two electron oxidation to form benzoquinoneimine. Third, acetaminophen is oxidized with P-450 to form hydroxylated intermediate (*N*-acetyl-*N*-hydroxy-*p*-aminophenol), subsequently followed by dehydration to form benzoquinoneimine. The main metabolite of **1** at the early stage of metabolism is most likely to be **2**, possessing the common *p*-aminophenol structure to acetaminophen. Therefore, **2** would be similarly oxidized to form the corresponding benzoquinoneimine as an intermediate. Actually, **2** could be chemically oxidized by lead tetraacetate very rapidly to yield the benzoquinoneimine. Additionally, Finley et al. (*30*) had discussed the specificity of reacting positions on benzene ring of *N*,*N*′-quinonediimine against a nucleophilic substitution. The regioselectivity of a nucleophilic addition to quinonediimine was examined by Hückel molecular orbital (HMO) theory, but a clear explanation could not be obtained due to the limitations of HMO calculations dealing only with π-electrons. However, assuming that all resonance integrals in a quinonediimine and its intermediates in nucleophilic addition were equal to the benzene resonance integral, it was proposed that the 1-, 3-, and 5-positions of *N*,*N*′-quinonediimine ring were highly susceptible to nucleophilic substitution. In our study, the fully optimized molecular geometries of **2** and its quinoneimine form in lower energy states were estimated by the AM1 method (*31*) in WINMOPAC program (version 2.0, Fujitsu, Ltd.). The distribution of the lowest unoccupied molecular orbital (LUMO) of **2** at the 5-position (12.1%) vs the 2- and 6-positions (15.9 and 2.2%, respectively) implied the higher reactivity to the nucleophilic attack at this position, while the examination of the LUMO of the quinoneimine form did not show any particular preference at the 5-position (23.4%) over the other ones (18.8 and 26.3% for the 2- and 6-positions, respectively). This might be elucidated by indicating the steric imposition on a substrate in the neighborhood of a reactive site of enzyme, which affects and/or determines the selectivity of reacting position on the phenyl ring of **2**. Actually, it has been reported in the metabolism of acetaminophen (*32*−*35*) that the 3- and 5-positions of quinoneimine are highly reactive to the nucleophilic attack by glutathione (GSH).

In summary, **1** primarily underwent *O*-deethylation at the 4-position of the phenyl ring to form **2**. Successively, **2** was likely to be converted via two electron oxidation to the corresponding benzoquinoneimine whose 5-position of the ring was attached by cysteine. Cysteine is the most probable nucleophile, since it is known to be formed by catabolism of the corresponding conjugates of GSH, a major ingredient in grape fruit (*36*). Then, the amino group of cysteine was considered to be transformed to the pyruvate structure as an intermediate by transaminase and finally to the thiolactic acid (**Figure 3**).

Incidentally, Lamoureux et al. first reported the existence of a thiolactic acid conjugate in various plants (*19*−*22*). They detected thiolactic acid conjugates in peanut, corn, cotton,

soybean, and spruce using mainly cell suspension culture. For example, EPTC, propachlor, and metolachlor were metabolized in cotton and corn to the corresponding (*O*-malonyl)thiolactic acid conjugates. However, the identification of the conjugate was only performed from the results of mass spectrometric analysis; thus, ambiguity remains for their chemical identities. Therefore, our study gives the first concrete evidence of the thiolactic acid conjugate by the definite identification by HPLC and TLC cochromatographies with the synthetic standards, together with LC-APCI-MS and NMR analyses. Additionally, as shown with the chemical structure of **6**, this is a new type of conjugation form in metabolites that has not been reported; that is, two natural products are conjugated within a different position of the same aglycone.

LITERATURE CITED

(1) Takahashi, J.; Nakamura, S.; Noguchi, H.; Kato, T.; Kamoshita, K. Fungicidal activity of *N*-phenylcarbamate against benzimidazole resistant fungi. *J. Pestic. Sci.* **1988**, *13*, 63−69.

(2) Takahashi, J.; Kirino, O.; Takayama, C.; Nakamura, S.; Noguchi, H.; Kato, T.; Kamoshita, K. Quantitative structure−activity relationships of fungicidal *N*-(3,4-diethoxyphenyl)carbamates. *J. Pestic. Sci.* **1988**, *13*, 587−593.

(3) Takahashi, J.; Kirino, O.; Takayama, C.; Nakamura, S.; Noguchi, H.; Kato, T.; Kamoshita, K. Quantitative structure−activity relationships of the fungicidal methyl *N*-phenylcarbamate. *Pestic. Biochem. Physiol.* **1988**, *30*, 262−271.

(4) James, C. S.; Prendeville, G. N. Metabolism of chlorpropham (isopropyl *m*-chlorocarbanilate) in various plant species. *J. Agric. Food Chem.* **1969**, *17*, 1257−1260.

(5) Still, G. G.; Mansager, E. R. Metabolism of isopropyl 3-chlorocarbanilate by soybean plants. *J. Agric. Food Chem.* **1971**, *19*, 879−884.

(6) Still, G. G.; Mansager, E. R. Aryl hydroxylation of isopropyl-3-chlorocarbanilate by soybean plants. *Phytochemistry* **1972**, *11*, 515−520.

(7) Still, G. G.; Mansager, E. R. Soybean shoot metabolism of isopropyl-3-chlorocarbanilate: Ortho and para aryl hydroxylation. *Pestic. Biochem. Physiol.* **1973**, *3*, 87−95.

(8) Still, G. G.; Mansager, E. R. Metabolism of isopropyl-3-chlorocarbanilate by cucumber plants. *J. Agric. Food Chem.* **1973**, *21*, 787−791.

(9) Still, G. G.; Rusness, D. G. *S*-cysteinyl-hydroxychlorpropham: Formation of the *S*-cysteinyl conjugate of isopropyl-3′-chloro-4′-hydroxycarbanilate in oat (*Avena sativa* L.). *Pestic. Biochem. Physiol.* **1977**, *7*, 210−219.

(10) Heikes, D. L. Mass spectral identification of a metabolite of chlorpropham in potatoes. *J. Agric. Food Chem.* **1985**, *33*, 246−249.

(11) Still, G. G.; Mansager, E. R. Metabolism of isopropyl carbanilate by soybean plants. *Pestic. Biochem. Physiol.* **1973**, *3*, 289−299.

(12) Still, G. G.; Mansager, E. R. Alfalfa metabolism of propham. *Pestic. Biochem. Physiol.* **1975**, *5*, 515−522.

(13) Zurqiyah, A. A.; Jordan, L. S.; Jolliffe, V. A. Metabolism of isopropyl carbanilate (propham) in alfalfa grown in nutrient solution. *Pestic. Biochem. Physiol.* **1976**, *6*, 35−45.

(14) Castello, A.; Marquet, J.; Moreno-Manas, M.; Sirera, X. The nucleophilic aromatic photosubstitution in photoaffinity labeling. A model study of a cycloheximide derivative. *Tetrahedron Lett.* **1985**, *26*, 2489−2492.

(15) Schmidt, R. R.; Zimmermann, P. Synthesis of glycosphingolipids and psychosines. *Angew. Chem., Int. Ed. Engl.* **1986**, *25*, 725−726.

(16) Hattori, K.; Takido, T.; Itabashi, K. The synthesis of thiols by use of *N*,*N*-dimethylthioformamide. *Nippon Kagaku Kaishi* **1979**, 101−105.

(17) Fernando, R. C.; Calder, I. C.; Ham, K. N. Studies on the mechanism of toxicity of acetaminophen. Synthesis and reactions of *N*-acetyl-2,6-dimethyl- and *N*-acetyl-3,5-dimethyl-*p*-benzoquinone imines. *J. Med. Chem.* **1980**, *23*, 1153−1158.

(18) Lee, H. H.; Palmer, B. D.; Denny, W. A. Reactivity of quinone imine and quinone diimine metabolites of the antitumor drug amsacrine and related compounds to nucleophiles. *J. Org. Chem.* **1988**, *53*, 6042−6047.

(19) Lamoureux, G. L.; Gouot, J. M.; Davis, D. G.; Rusness, D. G. Pentachloronitrobenzene metabolism in peanut. 3. Metabolism in peanut cell suspension cultures. *J. Agric. Food Chem.* **1981**, *29*, 996−1002.

(20) Lamoureux, G. L.; Rusness, D. G. EPTC metabolism in corn, cotton, and soybean: Identification of a novel metabolite derived from the metabolism of a glutathione conjugate. *J. Agric. Food Chem.* **1987**, *35*, 1−7.

(21) Lamoureux, G. L.; Rusness, D. G. Propachlor metabolism in soybean plants, excised soybean tissues, and soil. *Pestic. Biochem. Physiol.* **1989**, *34*, 187−204.

(22) Lamoureux, G. L.; Rusness, D. G.; Schröder, P.; Rennenberg, H. Diphenyl ether herbicide metabolism in a spruce cell suspension culture: The identification of two novel metabolites derived from a glutathione conjugate. *Pestic. Biochem. Physiol.* **1991**, *36*, 291−301.

(23) Hinson, J. A.; Monks, T. J.; Hong, M.; Highet, R. J.; Pohl, L. R. 3-(Glutathion-*S*-yl)acetaminophen: a biliary metabolite of acetaminophen. *Drug Metab. Dispos.* **1982**, *10*, 47−50.

(24) Morgan, E. T.; Koop, D. R.; Coon, M. J. Comparison of six rabbit liver cytochrome P-450 isozymes in formation of a reactive metabolite of acetaminophen. *Biochem. Biophys. Res. Commun.* **1983**, *112*, 8−13.

(25) Albano, E.; Rundgren, M.; Harvison, P. J.; Nelson, S. D.; Moldéus, P. Mechanism of *N*-acetyl-*p*-benzoquinone imine cytotoxicity. *Mol. Pharmacol.* **1985**, *28*, 306−311.

(26) Potter, D. W.; Miller, D. W.; Hinson, J. A. Horseradish peroxidase-catalyzed oxidation of acetaminophen to intermediates that form polymers or conjugate with glutathione. *Mol. Pharmacol.* **1986**, *29*, 155−162.

(27) Potter, D. W.; Hinson, J. A. Reactions of *N*-acetyl-*p*-benzoquinone imine with reduced glutathione, acetaminophen, and NADPH. *Mol. Pharmacol.* **1986**, *30*, 33−41.

(28) Potter, D. W.; Hinson, J. A. Mechanisms of acetaminophen oxidation to *N*-acetyl-*p*-benzoquinone imine by horseradish peroxidase and cytochrom P-450. *J. Biol. Chem.* **1987**, *262*, 966−973.

(29) Potter, D. W.; Hinson, J. A. The 1- and 2-electron oxidation of acetaminophen catalyzed by prostaglandin H synthase. *J. Biol. Chem.* **1987**, *262*, 974−980.

(30) Finley, T. K.; Tong, J. L. K. Quinonediimine and related compounds. In *The Chemistry of the Carbon−Nitrogen Double Bond*; Patai, S., Ed.; Interscience Publishers, London, 1970; pp 663−729.

(31) Dewar, M. J. S.; Zoebisch, E. G.; Healy, E. F.; Stewart, J. J. P. AM1: A new general purpose quantum mechanical molecular model. *J. Am. Chem. Soc.* **1985**, *107*, 3902−3909.

(32) Gemborys, M. W.; Gribble, G. W.; Mudge, G. H. Synthesis of *N*-hydroxyacetaminophen, a postulated toxic metabolite of acetaminophen, and its phenolic sulfate conjugate. *J. Med. Chem.* **1978**, *21*, 649−652.

(33) Miner, D. J.; Kissinger, P. T. Evidence for involvement of *N*-acetyl-*p*-quinoneimine in acetaminophen metabolism. *Biochem. Pharmacol.* **1979**, *28*, 3285−3290.

(34) Buckpitt, A. R.; Rollins, D. E.; Nelson, S. D.; Franklin, R. B.; Mitchell, J. R. Quantitative determination of the glutathione, cycteine, and *N*-acetyl cysteine conjugates of acetaminophen by high-pressure liquid chromatography. *Anal. Biochem.* **1977**, *83*, 168−177.

(35) Pascoe, G. A.; Calleman, C. J.; Baille, T. A. Identification of *S*-(2,5-dihydroxyphenyl)-cysteine and *S*-(2,5-dihydroxyphenyl)-*N*-acetyl-cysteine as urinary metabolites of acetaminophen in the mouse. Evidence for *p*-benzoquinone as a reactive intermediate in acetaminophen metabolism. *Chem.-Biol. Intract.* **1988**, *68*, 85−98.

(36) Park, S. K.; Boulton, R. B.; Noble, A. C. Automated HPLC analysis of glutathione and thiol-containing compounds in grape juice and wine using pre-column derivatization with fluorescence detection. *Food Chem*. **2000**, *68*, 475−480.

Received for review April 11, 2003. Revised manuscript received June 11, 2003. Accepted June 17, 2003.

JF034367+